

blood

2007 109: 3538-3543
Prepublished online Dec 27, 2006;
doi:10.1182/blood-2006-07-038588

Pathogenic proline mutation in the linker between spectrin repeats: disease caused by spectrin unfolding

Colin P. Johnson, Massimiliano Gaetani, Vanessa Ortiz, Nishant Bhasin, Sandy Harper, Patrick G. Gallagher, David W. Speicher and Dennis E. Discher

Updated information and services can be found at:

<http://bloodjournal.hematologylibrary.org/cgi/content/full/109/8/3538>

Articles on similar topics may be found in the following *Blood* collections:

[Cytoskeleton](#) (143 articles)

Information about reproducing this article in parts or in its entirety may be found online at:

http://bloodjournal.hematologylibrary.org/misc/rights.dtl#repub_requests

Information about ordering reprints may be found online at:

<http://bloodjournal.hematologylibrary.org/misc/rights.dtl#reprints>

Information about subscriptions and ASH membership may be found online at:

<http://bloodjournal.hematologylibrary.org/subscriptions/index.dtl>

Blood (print ISSN 0006-4971, online ISSN 1528-0020), is published semimonthly by the American Society of Hematology, 1900 M St, NW, Suite 200, Washington DC 20036.

Copyright 2007 by The American Society of Hematology; all rights reserved.



Pathogenic proline mutation in the linker between spectrin repeats: disease caused by spectrin unfolding

Colin P. Johnson,¹ Massimiliano Gaetani,² Vanessa Ortiz,¹ Nishant Bhasin,¹ Sandy Harper,² Patrick G. Gallagher,³ David W. Speicher,² and Dennis E. Discher¹

¹Molecular and Cell Biophysics Laboratory, University of Pennsylvania, Philadelphia, PA; ²Systems Biology Division, The Wistar Institute, Philadelphia, PA;

³Department of Pediatrics, Yale University School of Medicine, New Haven, CT

Pathogenic mutations in α and β spectrin result in a variety of syndromes, including hereditary elliptocytosis (HE), hereditary pyropoikilocytosis (HPP), and hereditary spherocytosis (HS). Although some mutations clearly lie at sites of interaction, such as the sites of spectrin α - β tetramer formation, a surprising number of HE-causing mutations have been identified within linker regions between distal spectrin repeats. Here we apply solution

structural and single molecule methods to the folding and stability of recombinant proteins consisting of the first 5 spectrin repeats of α -spectrin, comparing normal spectrin with a pathogenic linker mutation, Q471P, between repeats R4 and R5. Results show that the linker mutation destabilizes a significant fraction of the 5-repeat construct at 37°C, whereas the WT remains fully folded well above body temperature. In WT protein, helical linkers

propagate stability from one repeat to the next, but the mutation disrupts the stabilizing influence of adjacent repeats. The results suggest a molecular mechanism for the high frequency of disease caused by proline mutations in spectrin linkers. (Blood. 2007;109:3538-3543)

© 2007 by The American Society of Hematology

Introduction

Spectrin superfamily proteins have tandem arrays of 3-helix bundle spectrin repeats and are generally found in regions of cells that are exposed to mechanical stress.¹ Within erythrocytes, spectrin crosslinks F-actin into a resilient membrane network that normally allows these cells to distort reversibly for months under the high fluid shears of blood circulation.² Spectrin crosslinks consist of antiparallel heterotetramers of α -spectrin and β -spectrin that form staggered head-to-tail interactions between pairs of lateral α - β heterodimers (Figure 1A, inset). Crystal structures that have emerged in the past decade for a half-dozen tandem arrays of erythroid³⁻⁶ and nonerythroid spectrin⁷ repeats have been surprising and consistent in showing that linkers between spectrin repeats are continuous helices. Although such structures are obtained from static and dense-packed crystals that favor ordered states, solution studies⁸ and single-molecule measurements of forced extension⁹ also suggest cooperative coupling between erythroid spectrin repeats.

A wide range of mutations within erythrocyte spectrin perturbs cell structure and compromises the ability of the red blood cell to withstand mechanical forces, resulting in hereditary spherocytosis (HS), hereditary elliptocytosis (HE), or hereditary pyropoikilocytosis (HPP).^{10,11} Many of these mutations are in the N-terminal tetramerization site of the α -subunit or the β spectrin-ankyrin interaction. However, more than a dozen mutations distal to these sites have been linked to HE/HPP, and, of these, 7 mutations have been mapped to the linkers between repeats of α -spectrin. Five of these known mutations are prolines.¹¹ Given that it has recently become clear from studies of individual recombinant spectrin repeats that the melting temperatures of almost one third of the

repeats are at or below 37°C,¹² we hypothesized that proline-induced interruption of a helical linker would result in local nonhelicity within the linker,¹³ decoupling and destabilizing some spectrin repeats even at physiological temperatures and, thus, contributing to disease. Therefore, the continuity of helical linkers between tandem repeats may be critical to the overall mechanical properties of the erythrocyte membrane.

Here, the first 5 repeats of α -spectrin (aa 1-584) were expressed with either the wild-type (WT) sequence or the pathologic proline mutation Q471P. Although previous reports emphasize a disruption in RBC spectrin tetramers, we show that the mutant has equal affinity to WT in stable head-to-tail interactions with monomeric β -spectrin. However, thermal unfolding measured by several methods, including single-molecule forced extension and a cysteine-labeling technique, indicate a loss in structural stability of the Q471P mutant, even at 37°C. This is also predicted by temperature-dependent molecular dynamic simulations. The results thus demonstrate that erythroid spectrin with proline mutations in linkers between repeats can destabilize adjacent helical repeats and contribute directly to disease.

Materials and methods

Analysis of spectrin oligomers

Spectrin extracts were prepared at 4°C, as described,¹⁴ then concentrated to 12 to 14 mg/mL by vacuum dialysis against 10 mM Tris, 20 mM NaCl, 130 mM KCl, 1 mM EDTA, and 0.1 mM Na₃N, pH 7.4. Serial dilutions of spectrin in the same buffer were incubated for 3 hours at 30°C before

Submitted July 31, 2006; accepted December 3, 2006. Prepublished online as *Blood* First Edition Paper, December 27, 2006; DOI 10.1182/blood-2006-07-038588.

The online version of this article contains a data supplement.

An Inside *Blood* analysis of this article appears at the front of this issue.

The publication costs of this article were defrayed in part by page charge payment. Therefore, and solely to indicate this fact, this article is hereby marked "advertisement" in accordance with 18 USC section 1734.

© 2007 by The American Society of Hematology

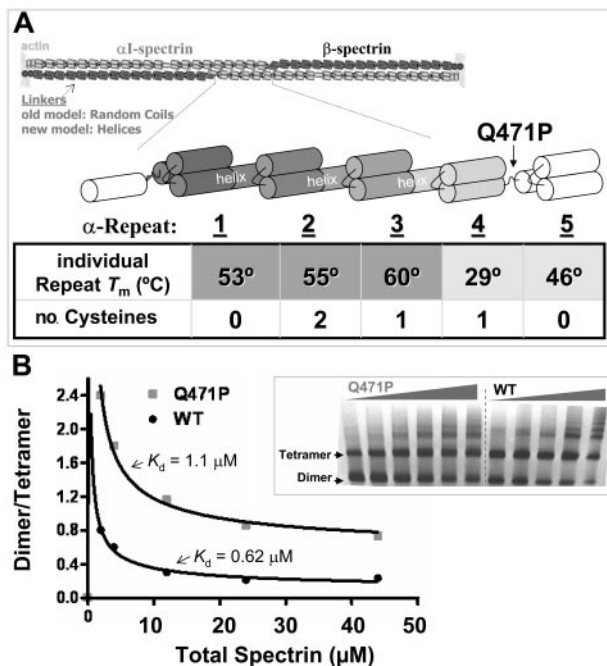


Figure 1. Spectrin structures and interactions and the anemia-causing linker mutant. (A) Antiparallel heterodimers of α -spectrin (light) and β -spectrin (dark) associate head to tail to form a tetramer that crosslinks F-actin at the red blood cell membrane. Linkers between repeats were originally thought to be random coils, but recent evidence suggests many are helical. Normal and mutant constructs of the α -spectrin N-terminus allow study of the effects of the pathogenic mutation Q471P, which is located in the linker between repeats α 4 and 5. The table lists the melting temperature of the individually expressed repeats² and the number of cysteines within each repeat. (B) Dimer-tetramer ratio for spectrin purified from control and patient blood, with model fits that yield a weaker dissociation constant $K_{d-tetramer}$ for the Q471P mutant (data not shown). (inset) A 2% to 4% gradient nondenaturing polyacrylamide gel of spectrin from control and patient erythrocytes. Lanes 1 to 5 contain WT sample spectrin concentrations of 11, 6, 3, 1, and 0.5 mg/dL. Lanes 6 to 11 contain hereditary elliptocytosis patient spectrin concentrations of 15, 11, 6, 3, 1, and 0.5 mg/dL.

electrophoresis. Spectrin oligomer formation was studied by electrophoresis of extracted spectrin on 2% to 4% gradient nondenaturing polyacrylamide slab gels at 4°C. Gels were electrophoresed at 50 V for 48 hours in buffer containing 40 mM Tris, 20 mM Na acetate, and 2 mM EDTA, pH 7.4. Quantitation of spectrin oligomers and peptides from Coomassie blue-stained acrylamide gels was performed by elution of excised gel slices with 1.0 mL of 25% pyridine for 3 to 4 days until the gel slice was colorless. Optical density of the eluted material at 700 nm was measured in a spectrophotometer.

Protein expression and purification of recombinant spectrin proteins

Residues 1-584 of α I spectrin and 1902-2084 of β I spectrin (repeats 16-17) were amplified by polymerase chain reaction (PCR) from erythrocyte spectrin cDNA clones.^{15,16} Site-directed mutagenesis was used to introduce Q471P in the 5-repeat α -spectrin construct (α 1-5). All constructs were expressed as glutathione *S*-transferase (GST) fusions using a pGEX-2T vector and DH5 α *Escherichia coli*. GST moiety was cleaved and purified from the supernatant by affinity chromatography, as described previously.¹⁷⁻¹⁹ The protein was concentrated using Centrprep concentrators (Millipore, Billerica, MA) and was further purified on G3000SW and G2000SW columns connected in series (60 \times 2.5 cm; Tosoh, Montgomeryville, AL) equilibrated with PBS plus 1 mM β -ME, 1 mM EDTA, and 0.15 mM PMSF, pH 7.4. Protein concentrations were determined by measuring OD₂₈₀ with ϵ_{280} calculated using the GPMW program.

Isothermal titration calorimetry

A VP-ITC isothermal titration calorimeter (MicroCal, Northampton, MA) was used for thermodynamic analysis of the binding between the α 1-5 WT and mutant and β 16-17 (residues 1902-2084). Samples were dialyzed in 2 steps (3 hours and overnight) against PBS. All samples and buffer were degassed under vacuum for 5 minutes before loading in the instrument. The reference cell was filled with the dialysate buffer, and the sample cell was filled with the dialysate for the control or with β 16-17 recombinant spectrin, used as titrated protein, at a concentration of 20 μ M; α 1-5 constructs were used as titrants in the syringe for control and sample experiments. Titration experiments were performed with stirring at 300 rpm and 25 to 29 injections of 10 μ L protein over 40 to 50 minutes. The area under each spike, representing the Δ heat for each injection, was integrated, and the control was subtracted from experimental data to correct for the dilution heat of the titrant protein into buffer. Integrated injections were then fit to a simple binding model with the use of nonlinear least square regression analysis. Measurements reported are for 25°C; measurements at 37°C gave weaker associations, as expected from past work, but mutant and normal controls were statistically the same.

Circular dichroism

Circular dichroism spectra were measured with the use of a spectrophotometer (J715; Jasco, Sydney, Australia) and a 1-mm path-length cell in PBS buffer (pH 7.5). The instrument was calibrated before sample measurement with *D*-10-camphorsulfonic acid. Three consecutive measurements at each temperature were made after allowing for thermoequilibrium and were averaged.

Differential scanning calorimetry

An MCS differential scanning calorimeter (DSC; MicroCal) was used to perform thermal denaturation studies on the α 1-5 and Q471P mutant. All samples and buffer were degassed for 5 minutes before they were loaded into the calorimeter. The dialysate buffer was used to fill the reference cell in buffer control and denaturation experiments, and the sample cell was filled with the dialysate buffer in control or protein sample at 0.5 to 1.0 mg/mL (6.5-13 μ M). All scans were taken from 20° to 90°C at a scanning rate of 90°C/h. Data analysis was performed using software provided with the instrument by subtracting the buffer control, subtracting the baseline fitted to the ends of the transitions, normalizing for the protein concentration, and curve-fitting using nonlinear least square regression analysis.

Molecular dynamics simulations

Atomistic-level molecular dynamics (MD) simulations were performed for the WT and the Q471P mutations using the 3D model of repeats 4-5, obtained from the Robetta website.²⁰⁻²⁷ The sequence for the spectrin repeats was obtained from the UniProtKB/Swiss-Prot Protein Knowledgebase, accession number P02549. Constructs were equilibrated in a box of explicit water for 10 nanoseconds at temperatures of 17°C, 27°C, or 37°C using the package NAMD²⁸ with the CHARMM27 force field.²⁹ Measurements of the root-mean-square-deviation (rmsd) of the positions of the backbone atoms show that after 5 nanoseconds, the protein structure reached equilibrium for all temperatures sampled; therefore, data were collected for the last 3 nanoseconds of simulation. Average helical content of the residues was calculated using the Lifson-Roig model,³⁰ by which a residue, *i*, was marked helical if, and only if, its backbone dihedral angle pair (ϕ_i , ψ_i) and its adjacent residue angle pairs (ϕ_{i-1} , ψ_{i-1} and ϕ_{i+1} , ψ_{i+1}) lay in the helical region $\phi = -65(\pm 35)^\circ$ and $\psi = -37(\pm 30)^\circ$. The average solvent-exposed area of the cysteine was calculated using the software MSMS³¹ for integration of molecular surfaces using a probe radius of 1.4 Å, a value typically used for water.

Cysteine labeling

Labeling of accessible cysteines was achieved by adding 13 μ L of 6 mM IAEDANS to a solution consisting of 0.5 mM TCEP and 200 μ L of 1 mg/mL protein in PBS, pH 7.5. Samples were allowed to react at 23°C,

30°C, 37°C, 45°C, 60°C, and 75°C for 45 minutes, after which the reaction was quenched by the addition of 10 μ L of 282 mM β -mercaptoethanol. After IAEDANS labeling, protein samples were run on a 12% Bis-Tris SDS gel, and the fluorescence intensity of the protein bands was imaged with a UV transilluminator. To account for disparities in sample loading, the gel was stained using Simply Blue colloidal stain and was digitally scanned. Fluorescence and blue stain intensities of each protein band were quantitated using Scion Image for Windows (<http://www.scioncorp.com>), and the fluorescence intensities were normalized by the blue stain intensity (sample loaded).

Atomic force microscopy measurements

Collection and analysis of single molecule unfolding measurements were carried out as described.⁹ Atomic force microscopy (AFM) was carried out on a Nanoscope IIIa Multimode (Digital Instruments, Santa Barbara, CA) equipped with a liquid cell and heater for temperature control. Protein density was adjusted so that less than 10% of tip-to-surface contact resulted in a protein unfolding event, and 5000 surface-to-tip measurements were made for each sample to ensure good statistics. Analysis of the force curves was conducted using a semiautomated visual analysis program written in C++.

Results

α - β Spectrin head-to-tail heterodimer interaction is unaffected by mutation

Effects of the Q471P mutation on head-to-tail interactions between the N-terminal α 1-5 construct (Figure 1A) and a C-terminal β -spectrin construct were first examined with the use of isothermal titration calorimetry (ITC). ITC measures protein binding through measurement of the heat given off during protein interaction at constant temperature. From the measured addition of heat as protein was added, the equilibrium dissociation constant, K_d , was determined, together with the heat or enthalpy of binding ΔH from a nonlinear curve fit. For the WT α 1-5 construct, $K_d = 0.44 \mu\text{M}$ (Figure S2, available on the *Blood* website; see the Supplemental Figures link at the top of the online article), and $\Delta H = -30 \text{ kcal/mol}$. Additionally, from the relationship $R\ln K_d = \Delta G = \Delta H - T\Delta S$, the interaction entropy $\Delta S = -73 \text{ cal/mol K}$ was calculated and indicated a significant and understandable increase in system order (water, protein, salt) upon association. These thermodynamic measures of interaction are close to those reported or estimated for full-length spectrin.³² The Q471P mutant also gave $K_d = 0.44 \mu\text{M}$, with similar ΔH and ΔS values (-35 kcal/mol and -87 cal/mol K). No significant difference in binding was thus detected between normal and mutant monomer.

Heterodimer association into full-length spectrin tetramers has been studied for decades, with one of the earliest studies by equilibrium ultracentrifugation indicating $K_{d\text{-tetramer}} = 0.5 \mu\text{M}$.³² This is similar to the dissociation constant for monomeric proteins, at least within the usual 10% to 15% error for protein concentration. Early work on the association of spectrin dimer extracted from human erythrocytes with the Q471P mutation suggested a weaker interaction of mutant full-length heterodimers, but no quantitative analysis was attempted.³³ Nondenaturing PAGE study of association was, therefore, repeated for normal and mutant spectrin from mutant and WT red cells, showing a 2-fold weaker association of mutant heterodimers into tetramers (Figure 1B). The control $K_{d\text{-tetramer}} = 0.62 \mu\text{M}$ was remarkably close to results cited, whereas the mutant gave $K_{d\text{-tetramer}} = 1.1 \mu\text{M}$. Because the defect was not in the monomeric association sites, we hypothesized that conforma-

tional perturbation within the mutant heterodimers might be the basis for weaker tetramer association.

Thermal denaturation in solution shows the mutant is less folded at 37°C

To examine the structural properties of the WT and mutant α 1-5 proteins, circular dichroism, tryptophan fluorescence, and calorimetric studies were conducted. CD spectra of the secondary structure for both constructs showed approximately 68% helical content at 19°C, which was consistent with past measurements on a range of spectrin constructs.¹² For the WT protein, this helicity increased slightly with temperature to more than 70%, up to 40°C. The Q471P mutant showed the opposite behavior: helicity decreased to approximately 55% at 37°C. The clear difference provided the first definitive evidence of destabilization resulting from a pathogenic linker mutation.

For both constructs, helicity decreased for temperatures higher than 40°C, with multistate unfolding. For the WT, a minor transition was seen first at $T_{mI} \approx 48^\circ\text{C}$, followed by the major transition at $T_{mII} \approx 59^\circ\text{C}$. Helicity loss, Δ , in each transition occurred in the ratio of $\Delta_I:\Delta_{II} = 13\%:34\% \approx 0.3:0.7$. This ratio suggested unfolding of one or 2 of the 5 WT repeats in the first transition. Two distinct melting temperatures might have been anticipated from past results³⁴ for the relevant tandem repeat constructs: α 4-5 had a $T_m = 41^\circ\text{C}$, whereas α 1-2 and α 2-3 had similar $T_m = 53^\circ\text{C}$ or 57°C . Figure 1 also tabulates T_m values that were measured recently¹⁴ for individual repeats, and again these were low for R4 and R5 (29°C and 46°C , respectively) and high for R1, R2, and R3 (53°C , 55°C , and 60°C , respectively). The comparisons clearly showed that placing repeats in tandem increased the stability above the simple average (eg, $\frac{1}{2}[T_{mR4} + T_{mR5}] < T_{m,\alpha4-5}$), which was consistent with cooperative stabilization by the linking helix.^{9,34} A tentative mechanism of unfolding the WT construct is, therefore, (I) for initial unfolding of the C-terminal α 4-5 repeats followed at higher temperature by (II) for cooperative unfolding of the N-terminal α 1-3 repeats. Destabilizing the linking helix between R4 and R5 with Q471P should primarily, as shown, have decreased and broadened transition-I for the mutant.

To assess the energetics of these transitions, differential scanning calorimetry (DSC) studies were also conducted on both constructs (Figure 2B). DSC on the WT recombinant protein showed 2 peaks in the heat capacity at similar transition temperatures (48°C and 60°C). By fitting a 2-state model to each peak, transition enthalpies of $\Delta H_I = 123 \text{ kcal/mol}$ and $\Delta H_{II} = 215 \text{ kcal/mol}$ were determined and appeared in the approximate proportion $\Delta H_I:\Delta H_{II} \approx 0.4:0.6$. This ratio provided perhaps the best

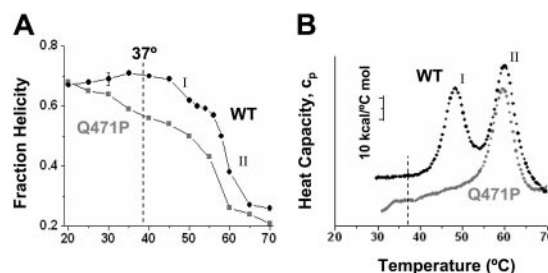


Figure 2. Thermal denaturation studies of the WT and Q471P mutant. WT and Q471P recombinant spectrin fraction folded as a function of temperature based on (A) circular dichroism and (B) DSC measurements all show a significant thermal destabilization of the Q471P mutant relative to the WT construct at or below 37°C.

evidence that the WT protein denatured first (I) through unfolding of the smaller α 4-5 domain followed by (II) unfolding of the larger α 1-3. For Q471P, the first transition appeared lost in a broad first peak. For the second transition with the mutant, however, estimates of T_{mII} and ΔH_{II} were only slightly lower than those of WT (59°C and 188 kcal/mol, respectively), suggesting that the α 1-3 in the mutant was relatively well folded. Solution structural studies were thus collectively clear in identifying a folding defect that arose with the pathogenic mutation Q471P.

Molecular dynamics demonstrates thermal unfolding of the mutant linker

Based on the structural evidence for coupling within α 4-5, the linker between repeats R4 and R5 was likely to be helical. For a better picture of this and the expected proline-induced effects in the putative helical linker, molecular dynamics simulations were performed on homology models of α 4-5 WT and the Q471P mutant. The linker for WT was indeed a stable helix after 8-nanosecond equilibration. For the mutant, in contrast, the helix was locally disordered immediately near the proline substitution. Shown in opaque yellow and in space-filling representation was the thiol in Cys⁴⁷⁵, which was approximately one helical turn away from the site of mutation and was more clearly exposed in the mutant.

At temperatures of 17°C, 27°C, and 37°C, helicity of the linker and solvent exposure of the thiol were quantified (Figure 3B). The relevant part of the linker on which to focus was identified based on the perturbation to helicity at 37°C in Q471P (Figure 3B, inset; blue residues in Figure 3A). Pro471 was at the center of the perturbation, as expected, and the loss in helical content extended several residues either side of it. At the low temperatures in simulation, the perturbation was minimal, consistent with solution studies (Figure 2). As with helicity at 37°C, however, Cys⁴⁷⁵ was less buried in the mutant. This increased solvent accessibility was

directly assessed with the novel use of small thiol-reactive reagents to probe thermal unfolding.

Cysteine labeling increases with thermal unfolding and more so for the mutant

Cysteines are relatively hydrophobic amino acids, and at least some of the 4 Cys residues of the α 1-5 construct were evidently buried. Unfolding is expected to increase cysteine exposure and, thus, to increase reactivity to thiol-reactive compounds, such as the fluorescent dye IAEDANS. Because the reaction exhibited only weak temperature dependence in denaturing solutions such as urea, changes in fluorescence labeling of the constructs with temperature (Figure 4A-B) largely reflected changes in the Cys-buried fraction. However, the first-order kinetics of labeling (Figure 4C) means that reaction rate differences resulting in differences in buried Cys generally decreased with time as label accumulated. Labeling of either construct was relatively low—up to 30°C (for 60 minutes)—but for temperatures of 37°C and higher, Cys was increasingly exposed and labeled, with greater labeling of Q471P than of WT up to full labeling of Cys at approximately 75°C (Figure 4B). Fits of labeling kinetics also revealed a 1.9-fold increased rate of labeling for the Q471P mutant (0.052 min⁻¹) relative to WT (0.099 min⁻¹), which was again indicative of increased Cys accessibility (Figure 4C). Because the only difference between the 2 recombinant constructs was the proline mutation localized near Cys, we hypothesized that the mutation locally disrupted linker helicity and exposed the nearby Cys. Mass spectrometry on 30-minute samples indeed detected considerable IAEDANS labeling of Cys⁴⁷⁵ in the Q471P mutant, but comparatively little labeling of WT was detected.

Just as Cys exposure increased with temperature, so did Trp hydration. Moreover, the mutant showed lower T_m than the WT (Figure S1A), yielding a picture similar to that of Cys labeling, but the latter appeared more definitive.

Single-molecule forced unfolding shows the mutant has fewer stable domains

Given that spectrin is a mechanically important protein to the red blood cell and that linker mutants, such as Q471P, lead to less stable membranes, we also sought to assess the mechanical effects of the Q471P linker mutation. Forced extension of single molecules by AFM was performed on both constructs. The characteristic sawtooth patterns of forced unfolding for the WT and the Q471P mutants at 23°C showed a maximum of 7 peaks ($N_{pk} = 1-7$), and this maximum was equivalent to the number of mechanically resilient spectrin domains plus initial and final desorption events (Figure 5A). The first and last peaks are not caused by protein unfolding.⁹ Therefore, we determined the number of unfoldable domains ($N_{pk} - 2$). The sawtooth thus implied up to 5 unfoldable domains for the WT and the Q471P mutants at 23°C, but the mutant showed 80% less such 5-domain events, and the mutant showed no such events at 30°C. Trends for 4-domain events, 3-domain events, and so on were similar. This simple, first analysis of forced extension thus implies that the proline linker mutant has fewer resilient domains under mechanical stress. Results are collectively consistent with the proline mutation destabilizing spectrin repeats.

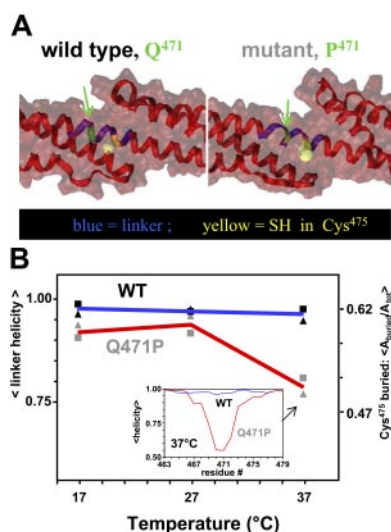


Figure 3. Molecular dynamics simulations show α 4-5 linker destabilization. (A) Snapshots of the α 4-5 linker (blue) for WT and mutant at 37°C. The mutated site and Cys⁴⁷⁵ are represented in green and yellow, respectively. Ribbon representations show a disruption of the helix in the linker of the mutant, whereas the molecular surface representation shows an increase in solvent-exposed area of the Cys. (B) Quantitation of Cys⁴⁷⁵ exposure (▲) and linker helical content (■) from molecular dynamics simulation. (inset) Normalized fraction of helical content along the backbones at 37°C. Note that compared with WT (blue line), the Q471P mutant (red line) shows considerable loss in helicity (approximately 40%) in the linker region. Arrows denote area of helix altered by proline mutation.

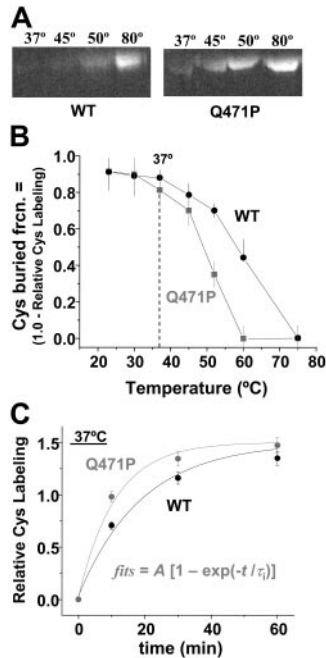


Figure 4. Cysteine labeling compared with temperature for mutant and WT. (A) SDS-PAGE followed by fluorescence imaging of IAEDANS-labeled proteins illustrates an increase in Cys labeling at lower temperatures for the mutant. (B) Unlabeled Cys compared with temperature after 60-minute reaction. Splayed curves resemble the unfolding curves of Figure 2, with significant differences in labeling at temperatures higher than 30°C. (C) IAEDANS reaction kinetics of WT and Q471P with associated fits. First-order reaction rate fits to the data demonstrate a 1.9-fold faster rate of reaction for Q471P than for WT.

Discussion

Thermal denaturation studies here suggest that the WT α 1-5 construct unfolds in a partially cooperative 3-state manner. Cooperativity between other spectrin repeats is increasingly clear in solution studies and single-molecule force measurements of multirepeat stability.^{9,12} The single aa mutation at Q471P uncoupled repeats (Figures 1A, 3), limiting the cooperativity between repeats and leading to a divergence in unfolding pathways (Figure 6A). By plotting helicity versus Cys labeling for both constructs and using temperature to create parameters for the pathways, the WT construct showed no significant perturbation of structure up to approximately 37°C, after which Cys exposure increased (above the diagonal) before significant loss of helical secondary structure occurred greater than approximately 42°C. The Q471P showed clearly opposite behavior (below the diagonal) to approximately 37°C. Although the helicity measurements were equilibrium measurements and the temperature-dependent Cys exposure results (Figure 4B) were kinetic snapshots (Figure 4C), the clear differences in initial unfolding suggest independent and distinct multistate unfolding pathways. Additional analyses of fractional helicity compared with Trp exposure showed a similar divergence (Figure S1B) and highlighted an initial loss in helicity for the mutant that preceded other changes.

Based on the localized thermal instability seen in molecular dynamics simulations and the weaker mechanical stability detected in force measurements, the proline mutation lowered the thermal stability of the α 4-5 linker, resulting in a loss of structure at physiological temperature (Figure 3). This loss in linker helicity limited the stabilizing effects of R5 on R4 and led to independent unfolding of R4 ($T_m = 29^\circ\text{C}^{11}$). Linker coupling generally appears

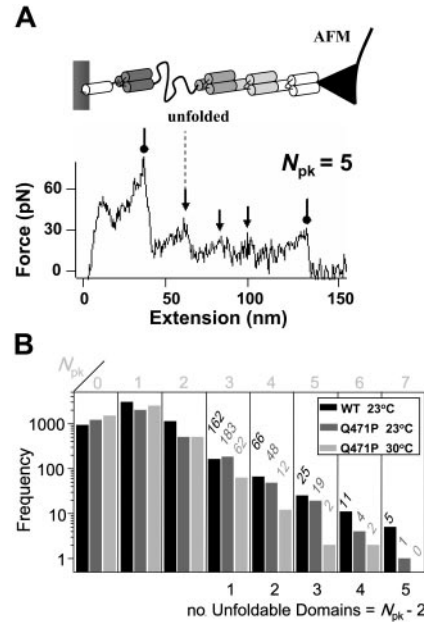


Figure 5. Domain numbers under mechanical stress. (A) Schematic diagram of AFM-forced unfolding with a single repeat shown unfolded. Such unfolding yields a single peak (arrows) in the sawtooth-shaped force-extension plot; the first and last peaks (circles) correspond to desorption of the protein from either the surface or the AFM tip. (B) Frequency of occurrence for unfolding spectrin domains ($N_{pk}-2$). The mutant shows fewer high N_{pk} sawtooth patterns, indicating a relative loss of domain structure.

to be sequence specific rather than based on helical content alone,³⁵ and steered molecular dynamics studies on related repeats have found this coupling to be largely based on the sequestration of linker residues from water.³⁶ Exposure of the hydrophobic residue side-chains within this region lead to a loss in the tertiary structure of the linker and the repeats.

Human erythrocytes with the Q471P mutation show a shift in the tetramer-dimer equilibrium toward heterodimers, with almost a 2-fold weaker $K_{d-tetramer}$ for the mutant. However, our ITC experiments on dimers demonstrated no effect on head-to-tail dimerization of monomeric α 1-5 and β 16-17 recombinant peptides. We propose that unfolding of repeats affects association into tetramer because of the staggered nature of dimerization (Figure 1A, inset).

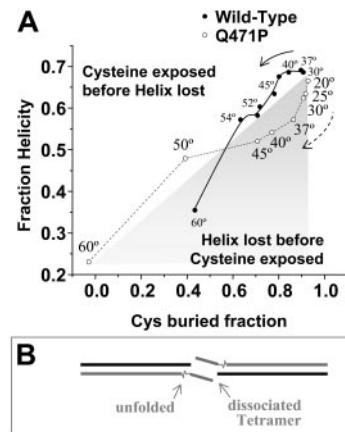


Figure 6. Proline mutation alters folding state. (A) Plot of helicity compared with fraction unlabeled cysteine at temperatures ranging from 20°C to 60°C reveals divergent unfolding pathways on mutation (B) The reduced structural stability of the mutant is speculated to add flexibility and to increase entropy in destabilizing the α - β association in the tetramer.

In the tetramer, α 4-5 repeats are proximal to the dimerization site in the adjacent spectrin chain so that unfolded, flexible chains could enhance the configuration space of the dissociated state or could sterically inhibit association, just as sterics limits thiol reactivity (Figure 4). The flexibility would shift the tetramer–dimer distribution toward dissociation by decreasing the on-rate (Figure 6B). With this in mind, it becomes clear why a single amino acid mutation in a normally ordered linker can result in the shape changes and reduced erythrocyte membrane integrity associated with hemolytic elliptocytosis.

Acknowledgments

Supported by funding from National Institutes of Health grants HL65448 (P.G.G.) and HL38794, the National Institutes of Health–National Heart, Lung and Blood Institute (D.E.D.), NCI Cancer Core grant CA10815, and the Commonwealth Universal Research Enhancement Program, Pennsylvania Department of Health (D.W.S.).

References

- Bennett V, Gilligan DM. The spectrin-based membrane skeleton and micron-scale organization of the plasma membrane. *Annu Rev Cell Biol.* 1993; 9:27-66.
- Mohandas N, Evans E. Mechanical properties of the red cell membrane in relation to molecular structure and genetic defects. *Annu Rev Biophys Biomol Struct.* 1994;23:787-818.
- Kusunoki H, Minasov G, Macdonald RI, Mondragon A. Independent movement, dimerization and stability of tandem repeats of chicken brain alpha-spectrin. *J Mol Biol.* 2004;344:495-511.
- Ylanne J, Scheffzek K, Young P, Saraste M. Crystal structure of the alpha-actinin rod reveals an extensive torsional twist. *Structure.* 2001;3:597-604.
- Djinovic-Carugo K, Young P, Gautel M, Saraste M. Structure of the alpha-actinin rod: molecular basis for cross-linking of actin filaments. *Cell.* 1999;98:537-546.
- Grum, VL, Li D, MacDonald RI, Mondragon A. Structures of two repeats of spectrin suggest models of flexibility. *Cell.* 1999;98:523-535.
- Kusunoki H, MacDonald RI, Mondragon A. Structural insights into the stability and flexibility of unusual erythroid spectrin repeats. *Structure.* 2004; 12:645-656.
- Batey S, Scott KA, Clarke J. Complex folding kinetics of a multidomain protein. *Biophys J.* 2005; 90:2120-2130.
- Law R, Liao G, Harper S, Yang G, Speicher DW, Discher D. Pathway shifts and thermal softening in temperature-coupled forced unfolding of spectrin domains. *Biophys J.* 2003;85:3286-3293.
- Iolascon A, Perrotta S, Stewart GW. Red blood cell membrane defects. *Rev Clin Exp Hematol.* 2003;7:22-56.
- Giorgi M, Cianci CD, Gallagher PG, Morrow JS. Spectrin oligomerization is cooperatively coupled to membrane assembly: a linkage targeted by many hereditary hemolytic anemias? *Exp Mol Pathol.* 2001;70:215-230.
- An X, Guo X, Zhang X, et al. Conformational stabilities of the structural repeats of erythroid spectrin and their functional implications. *J Biol Chem.* 2006;281:10527-10532.
- Speicher DW, Marchesi VT. Erythrocyte spectrin is comprised of many homologous triple helical segments. *Nature.* 1984;311:177-180.
- Morrow J, Haigh W, Marchesi VT. Spectrin oligomers: a structural feature of the erythrocyte cytoskeleton. *J Supramol Struct.* 1981;17:275-287.
- Sahr KE, Laurila P, Kotula L, et al. The complete cDNA and polypeptide sequences of human erythroid alpha-spectrin. *J Biol Chem.* 1990;265: 4434-4443.
- Winkelmann JC, Chang JG, Tse WT, Scarpa AL, Marchesi VT, Forget BG. Full-length sequence of the cDNA for human erythroid beta-spectrin. *J Biol Chem.* 1990;265:11827-11832.
- Wilmotte R, Harper SL, Ursitti JA, Marechal J, Delaunay J, Speicher DW. The exon 46-encoded sequence is essential for stability of human erythroid alpha-spectrin and heterodimer formation. *Blood.* 1997;90:4188-4196.
- Begg GE, Harper SL, Morris MB, Speicher DW. Initiation of spectrin dimerization involves complementary electrostatic interactions between paired triple-helical bundles. *J Biol Chem.* 2000; 275:3279-3287.
- Harper SL, Begg GE, Speicher DW. Role of terminal nonhomologous domains in initiation of human red cell spectrin dimerization. *Biochemistry.* 2001;40:9935-9943.
- Scott MD, Frydman J. Aberrant protein folding as the molecular basis of cancer. *Methods Mol Biol.* 2003;232:2037-2049.
- Kim DE, Chivian D, Baker D. Protein structure prediction and analysis using the Robetta server. *Nucleic Acids Res.* 2004;32:W526-W531.
- Chivian D, Kim DE, Malmstrom L, et al. Automated prediction of CASP-5 structures using the Robetta server. *Proteins.* 2003;53(suppl 6):524-533.
- Bonneau R, Strauss CE, Rohl CA, et al. De novo prediction of three-dimensional structures for major protein families. *J Mol Biol.* 2002;322:65-78.
- Bonneau R, Tsai J, Ruczinski I, et al. Rosetta in CASP4: progress in ab initio protein structure prediction. *Proteins.* 2001;(suppl 5):119-126.
- Simons KT, Ruczinski I, Kooperberg C, Fox B, Bystroff C, Baker D. Improved recognition of native-like protein structures using a combination of sequence-dependent and sequence-independent features of proteins. *Proteins.* 1999;34:82-95.
- Simons KT, Kooperberg C, Huang E, Baker D. Assembly of protein tertiary structures from fragments with similar local sequences using simulated annealing and Bayesian scoring functions. *J Mol Biol.* 1997;268:209-225.
- Chivian D, Kim DE, Malmstrom L, Schonbrun J, Rohl CA, Baker D. Prediction of CASP6 structures using automated Robetta protocols. *Proteins.* 2005;61(suppl 7):157-166.
- Kale L, Skeel R, Bhandarkar M, et al. Greater scalability for parallel molecular dynamics. *J Comput Phys.* 1999;151:283-312.
- MacKerell AD, Bashford D, Bellott M, et al. All-atom empirical potential for molecular modeling and dynamics studies of proteins. *J Phys Chem B.* 1998;102:3586-3616.
- Lifson S. J. On the theory of helix–coil transition in polypeptides. *Chem Phys.* 1961;34:1963-1974.
- Sanner MF, Olson AJ, Spehner JC. Reduced surface: an efficient way to compute molecular surfaces. *Biopolymers.* 1996;38:305-320.
- Ungewickell E, Gratzner W. Self-association of human spectrin: a thermodynamic and kinetic study. *Eur J Biochem.* 1978;88:379-385.
- Marchesi SL, Letsinger JT, Speicher DW, et al. Mutant forms of spectrin alpha-subunits in hereditary elliptocytosis. *J Clin Invest.* 1987;80:191-198.
- MacDonald RI, Cummings JA. Stabilities of folding of clustered, two-repeat fragments of spectrin reveal a potential hinge in the human erythroid spectrin tetramer. *Proc Natl Acad Sci U S A.* 2003;101:1502-1507.
- Batey S, Randles LG, Steward A, Clarke J. Cooperative folding in a multi-domain protein. *J Mol Biol.* 2005;349:1045-1059.
- Ortiz V, Nielsen SO, Klein ML, Discher DE. Unfolding a linker between helical repeats. *J Mol Biol.* 2005;349:638-647.

Authorship

Contribution: D.E.D., P.G., and D.W.S. designed the research, analyzed the data, and wrote the paper. C.P.J., G.M., V.O., N.B., and S.H. performed the research and analyzed the data.

Conflict-of-interest disclosure: The authors declare no competing financial interests.

C.P.J. and G.M. contributed equally to this article.

This article is dedicated to the memory of Dr Sally Marchesi for her pioneering investigations into the molecular basis of spectrin pathologies.

Correspondence: Patrick G. Gallagher, Department of Medicine, Yale University School of Medicine, 333 Cedar St, New Haven, CT 06520; e-mail: patrick.gallagher@yale.edu; David W. Speicher, The Wistar Institute, 3601 Spruce St, Philadelphia, PA 19104; e-mail: speicher@wistar.org; and Dennis E. Discher, Molecular and Cell Biophysics Laboratory, University of Pennsylvania, 3699 Market St, Philadelphia, PA19104; e-mail: discher@seas.upenn.edu.